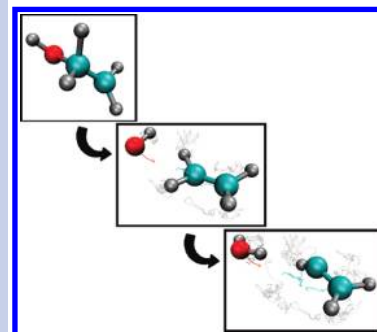


Roaming Pathway Leading to Unexpected Water + Vinyl Products in C₂H₄OH Dissociation

Eugene Kamarchik,^{*,†,‡} Lucas Koziol,[†] Hanna Reisler,[†] Joel M. Bowman,[‡] and Anna I. Krylov[†][†]Department of Chemistry, University of Southern California, Los Angeles, California 90089-0482, United States, and [‡]Cherry L. Emerson Center for Scientific Computation, Department of Chemistry, Emory University, Atlanta, Georgia 30322, United States

ABSTRACT We report molecular dynamics simulations of the unimolecular dissociation of energetic C₂H₄OH radicals using a full-dimensional potential energy surface (PES) fit to density functional theory (DFT) and coupled cluster (CCSD) calculations. Quasiclassical trajectories are initiated on the surface using microcanonical sampling at a total energy of 85.0 kcal/mol (44.1 kcal/mol relative to the zero-point energy). The trajectories reveal a roaming channel leading to the formation of water. The transition state (TS) corresponding to direct water production is energetically inaccessible. However, the roaming pathway finds a lower-energy path via frustrated dissociation to hydroxyl that makes water + vinyl production feasible. The trajectory calculations suggest that the roaming pathway constitutes a minor (a few percent) channel of the overall C₂H₄OH dissociation. The mechanism of the roaming reaction is analyzed in terms of the geometric proximity of the TSs leading to OH loss and internal abstraction as well as the partitioning of vibrational energy into different modes.

SECTION Dynamics, Clusters, Excited States



Recently, there has been considerable interest in roaming processes in molecular dissociations. In these processes, two incipient radicals may spend several hundred femtoseconds at separations of between 3 and 4 Å before sampling an orientation that leads to an internal abstraction leading to other products. Because such large radical–radical distances place the nascent fragments on flat regions of the potential energy surface (PES), the fragments move almost independently of each other and are able to sample many different relative orientations, hence the term “roaming”.¹ In several recent combined theory and experiment papers, it has been demonstrated that under certain conditions, the two radicals may roam until they reach an attractive portion of the PES that leads to internal abstraction and then to molecular products. According to these studies, roaming-type mechanisms should, in fact, be quite general in molecules for which an initially frustrated dissociation can be followed by a barrierless internal abstraction.^{2–7} While most often roaming accounts for only a minor fraction of the total products, under favorable conditions, roaming may even be the dominant mechanism and certainly needs to be taken into account for a complete picture of molecular dissociation.

Theoretical studies of roaming in acetaldehyde and formaldehyde dissociation have identified certain conditions that favor the existence of and branching to a roaming channel. In formaldehyde, the molecular products H₂ and CO can be formed both via a direct pathway and a roaming pathway that involves partial dissociation to H + HCO. For roaming, the correct amount of vibrational energy must be sequestered in internal motions of HCO, and the energy

in the dissociation coordinate must be within a 100 cm⁻¹ range of the threshold for radical dissociation. In this range, the hydrogen atom is free to make large excursions away from HCO, and it can access the region of the PES where it can abstract another hydrogen.^{1,2,8,9} In acetaldehyde, a similar pathway leads to the formation of CH₄ + CO through a roaming mechanism involving CH₃ and HCO. It is believed that the proximity of the energy thresholds for the direct formation of CH₄ + CO and for the loose roaming TS favor the roaming reaction.^{4,10–12}

Previous roaming studies have focused primarily on the dissociation of closed-shell molecules into two radicals. In this paper, we present a theoretical study that demonstrates the existence of roaming when the initial dissociation creates a radical and a closed-shell molecule. Provided that there exist regions of the PES that allow the initial fragments to spend sufficient time in reasonable proximity, conditions may exist that allow access to geometries favorable for internal abstraction. Such conditions appear to exist in the dissociation of the 2-hydroxyethyl radical (CH₂CH₂OH). The lowest dissociation pathway, which leads to OH and C₂H₄, contains a hydrogen-bonded complex. This attractive interaction allows the OH radical to roam a region of the PES near the ethene product and potentially abstract a H atom, yielding H₂O + C₂H₃. The abstraction OH + C₂H₄ → H₂O + C₂H₃ is exothermic but proceeds over a barrier of 5–6 kcal/mol.^{13–16} Our

Received Date: August 20, 2010

Accepted Date: September 28, 2010

Table 1. Selected Stationary Points on the PES^a

label	location	potential (kcal/mol)	curvature (cm ⁻¹)	total (kcal/mol)	RQCIT/QCI ¹⁴ (kcal/mol)
M1	CH ₂ CH ₂ OH	0.00	NA	0.00	0.00
TS1	CH ₂ CH ₂ OH → CH ₂ CH ₂ ·OH	28.40	87.3	25.95	26.8
M2	CH ₂ CH ₂ ·OH	26.06	NA	24.75	24.3
P1	CH ₂ CH ₂ + OH	27.92	NA	26.66	26.2
TS2	CH ₂ CH ₂ OH → CH ₂ CHOH + H	37.24	925.4	33.37	33.1
P2	CH ₂ CHOH + H	33.13	NA	28.20	27.2
TS3	CH ₂ CH ₂ OH → CH ₃ CHOH	39.96	1337.9	37.53	38.3
M3	CH ₃ CHOH	-8.46	NA	-8.58	-6.5
TS4	CH ₂ CH ₂ OH → CH ₃ CH ₂ O	34.4	2017.9	32.48	31.9
M4	CH ₃ CH ₂ O	-0.65	NA	0.24	3.4
TS5	CH ₂ CH ₂ + OH → CH ₂ CH + H ₂ O	30.24	1174.6	30.50	31.1
P3	CH ₂ CH + H ₂ O	16.88	NA	13.09	17.9

^a Minima are labeled with the letter M, transition states are labelled with TS, and products are labelled with P. For the transition points, curvature refers to the frequency of the imaginary normal mode. All potential energies are given relative to the potential energy at M1 ($E = -154.434157$ hartree), and all total energies are given relative to the total energy, including the zero-point energy, at M1 ($E = -154.368929$ hartree). The values calculated by Senosiain et al. are also shown.¹⁴

calculations show that when there is proper energy partitioning between the C₂H₄ fragment and the dissociation coordinate, a fraction of the nascent fragments can react to give water plus vinyl.

The chemistry of hydroxyethyl radicals and their isomerization and dissociation products is important in combustion and atmospheric chemistry.^{13,14,16–39} The 2-hydroxyethyl radical is an intermediate in the OH + C₂H₄ reaction^{18,26,29,32,33} and has been stabilized at low reaction temperatures.^{14,23–26,28,30,31,36} The major decomposition channel of CH₂CH₂OH in its ground electronic state is CH₂·CH₂ + OH.^{14,18,26,27,29,33} Minor decomposition channels appear at higher energies and include H + vinyl alcohol (ethenol), H + acetaldehyde, and CH₃ + formaldehyde, with the latter two being generated via isomerization to the ethoxy radical.^{14,33,40} Experimentally, CH₂CH₂OH radicals can be produced efficiently by photolysis of haloethanols,^{19–22,34,40} generating rovibrationally excited 2-hydroxyethyl radicals with maximum energies that exceed the dissociation threshold.

Numerous theoretical studies of the ground-state decomposition and isomerization of CH₂CH₂OH have been published.^{13,14,16,30,35,37–39,41–44} These studies, none of which employed dynamics calculations, explored limited regions of the PES. One interesting finding was that the lowest dissociation pathway, which leads to OH and C₂H₄ products, involves a weakly hydrogen-bonded complex, which plays an important role in the work reported here.

Motivated by recent experiments, we undertook a full-dimensional dynamics study of the decomposition of CH₂CH₂·OH. In doing so, we discovered that the hydrogen-bonding interaction allows the OH radical to roam a region of the PES near the ethene product and to abstract a H atom, yielding H₂O + C₂H₃. The barrier to the direct formation of water from CH₂CH₂OH (i.e., through a TS connecting CH₂CH₂OH with H₂O + C₂H₃) is much higher than the 5–6 kcal/mol barrier for abstraction, about 40 kcal/mol above the OH + C₂H₄ energy.¹³ The high barrier has led previous studies to neglect the possibility of water formation. Our calculations

show that when there is a favorable energy partitioning between C₂H₄ and the dissociation coordinate, some nascent fragments can react to give water plus vinyl via a roaming mechanism.

To investigate the dissociation dynamics of the C₂H₄OH radical, we constructed a full-dimensional PES. The surface is a permutationally invariant fit to CCSD/cc-pVDZ energies located near the minima and B3LYP/cc-pVDZ points describing the various dissociation and product channels. All calculations were performed using Q-Chem.⁴⁵ The full surface was fit to over 50 000 ab initio data energies, which were distributed among all possible minima, products, and fragment channels (see Supporting Information for details). We used high-order permutationally invariant polynomials based on Morse variables⁴⁶ to fit the surface. Several fits were performed using different combinations of the data and fitting parameters in order to verify the robustness of the PES. All of the results presented below, however, are from the optimum fit.

To validate that the fitted PES reproduces key stationary points (extensively characterized in ref 14), we performed geometry optimizations and several TS searches to locate the stationary points on the fitted PES. TSs along dissociation pathways were located by minimizing all remaining degrees of freedom while scanning along a single internal coordinate that was held at a fixed value, and they were verified by a calculation of the harmonic frequencies and the identification of a single imaginary frequency mode. We found that our PES contains all of the relevant minima, TSs, and products. A list of stationary points that are relevant to the isomerization or decomposition of CH₂CH₂OH is shown in Table 1 (see Supporting Information for details).

The PES contains TSs and product channels associated with all pathways for CH₂CH₂OH dissociation up to approximately 60 kcal/mol above M1. A complete listing of the stationary points including comparisons to previous works can be found in the Supporting Information. Here, we focus primarily on the regions of space associated with TS1, M2, and TS5, which are shown in Figure 1.

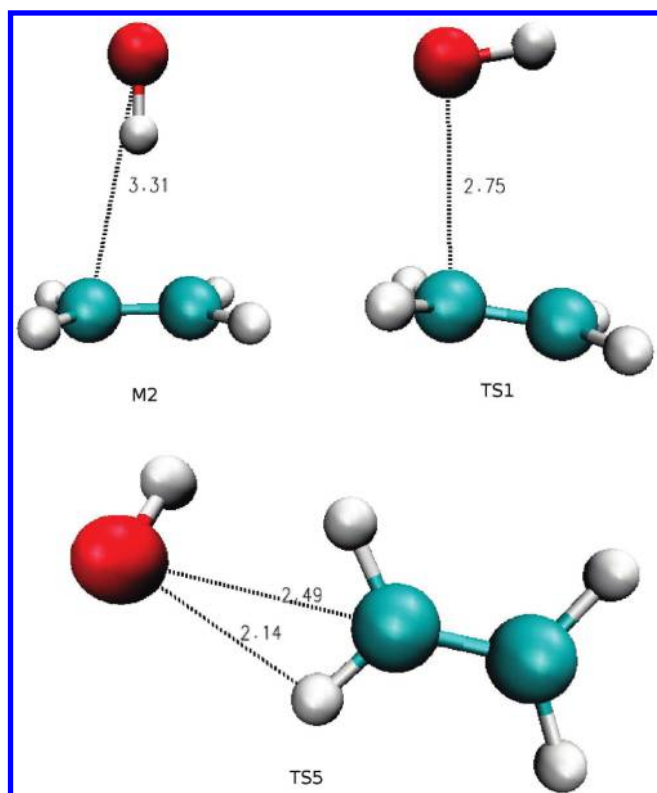
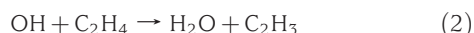


Figure 1. The transition states TS1 (OH loss channel) and TS5 (abstraction channel) and the hydrogen-bonded complex M2. All distances are given in Å.

Among multiple dissociation channels available to C_2H_4-OH ,¹⁴ we focus on the following



Reaction 1 proceeds via the hydrogen-bonded intermediate M2. The TS connecting CH_2CH_2OH and M2, TS1, has characteristics of both product and reactant states. The hydroxyl is at a distance of $r(C-O) = 2.75$ Å, but its orientation relative to CH_2CH_2 is similar to that in CH_2CH_2OH . The CH_2CH_2 fragment is already nearly planar and resembles ethene. However, the orbital structure is distorted and, unlike the hydrogen-bonded complex, does not have a fully formed π system (see below). M2 has a fully formed ethene fragment, characterized by its π highest occupied molecular orbital (HOMO), with the OH slightly further away, $r(C-O) = 3.3$ Å, oriented so that its hydrogen atom is pointing into the π cloud of ethene. On our PES, the energy required to completely dissociate to OH and ethene is slightly higher than the energy of TS1, allowing OH to become temporarily trapped, consistent with previous calculations.^{13,14} We also find a small barrier, <0.5 kcal/mol, separating M2 from P1, which we think is an artifact of the fitting procedure and small enough to not materially affect our calculations. Finally, the TS corresponding to hydrogen abstraction by the hydroxyl, TS5, has a similar $r(C-O) = 2.5$ Å distance to TS1, but with OH rotated about the ethene so that a lone pair on the oxygen

can interact with a hydrogen on the ethene (Figure 1). TS5 is 5–6 kcal/mol higher in energy than TS1. While TS5 is tighter than TS1, as seen from the imaginary frequencies, there is some flexibility, particularly with respect to rotation of the dihedral angle of the H atom in the hydroxyl group.¹³ Although TS5 and TS1 are connected by a monotonically decreasing path, this path does not correspond to an intrinsic reaction coordinate and is less steep than the path connecting TS5 with P3 and P1.

We performed quasiclassical trajectory calculations using the PES. The initial conditions were chosen such that the total vibrational energy, including zero-point contributions, was 85.0 kcal/mol. Removing the zero-point portion left the molecule with 44.1 kcal/mol of internal energy, which is near the upper limit obtained by the photodissociation of 2-bromoethanol ($BrCH_2CH_2OH$) with 193 nm light.^{22,34} The energy was distributed randomly among the normal modes, calculated at M1, with the constraint that all modes had to contain at least zero-point energy (ZPE). On the basis of the energy, each mode was assigned a vibrational quantum number based on the harmonic approximation, which was then used to generate a random phase for the normal mode. After projecting out angular and translational velocities, the displacements and momenta were then iteratively scaled to achieve the desired energy. For a select number of trajectories, we also performed ab initio direct dynamics with B3LYP/aug-cc-pVDZ using MOLPRO.⁴⁷

The PES was designed primarily to explore the high-dimensional space describing 2-hydroxyethyl dissociation. While the surface contains all of the relevant stationary points and is similar to the PES published recently near the minimum,³⁵ the high-energy saddle points are typically only within 2–3 kcal/mol of previous theoretical results.^{13,14} Thus, the surface should be able to qualitatively reproduce the dissociation dynamics and explain mechanisms but is not yet sufficiently accurate to quantitatively predict branching ratios.

The dynamical coupling among different vibrational modes leads to long-lived trajectories that typically need to be propagated for tens or hundreds of picoseconds before dissociating. At 44 kcal/mol of internal energy (relative to the ZPE), the major channel is dissociation to OH + ethene, with small fractions of products in all three other channels. This qualitatively agrees with experimental results.^{14,20–22,33,40} A feature which has not been predicted by statistical methods, however, is the presence of a small, but appreciable, fraction of H_2O in the products. As the TS leading to direct formation of water is above the energy available in the calculations, as discussed above, this dissociation channel must be produced by an alternative mechanism, as detailed below.

While statistical models are useful in predicting branching ratios and offering insight into reaction mechanisms, they are usually insensitive to structures of the PES away from TSs and products, which may play a significant role in certain reactions. Importantly, it is still unknown whether statistical models are capable of treating roaming mechanisms in this case. Provided one can locate appropriate dividing surfaces and properly count the density of states, a statistical approach may be successful. Starting from CH_2CH_2OH , the channel

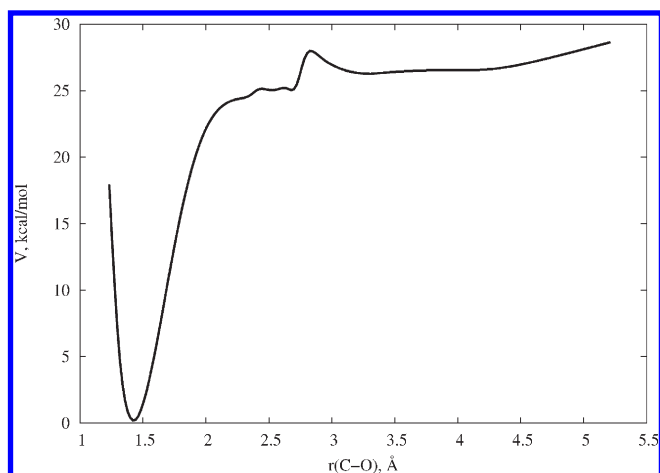


Figure 2. Relaxed energy path corresponding to loss of OH in the dissociation $\text{CH}_2\text{CH}_2\text{OH} \rightarrow \text{CH}_2\text{CH}_2 + \text{OH}$. The transition state is relatively flat, and there is a weakly bound hydrogen-bonded complex occurring at $r(\text{C}-\text{O}) \approx 3 \text{ \AA}$.

leading to direct water loss has a TS that requires over 70 kcal/mol of internal energy, which precludes access to this channel at our energy.^{15–16} We find, however, that water can be eliminated via a mechanism that involves frustrated dissociation of OH, followed by internal abstraction, namely, a roaming mechanism. The relaxed energy pathway leading to OH + ethene, computed by pulling the O away and allowing all other degrees of freedom to relax, evolves via a weakly bound complex and includes a fairly flat, shelf-like region between $r(\text{C}-\text{O}) = 2.0$ and 2.75 \AA . Near TS1, the OH fragment undergoes a large relative rotation, leading to a bump in the energy when viewed along the $r(\text{C}-\text{O})$ coordinate. Prior to this rotation, the OH fragment is aligned such that the H atom is pointing away from the ethene, while afterward, the H atom points toward the ethene. The flat region around TS1 allows the departing OH fragment to either get trapped near the ethene or return after venturing to significantly extended distances (Figure 2). While the fragments are trapped briefly in this region, the OH may abstract a hydrogen from ethene, thus forming the energetically more stable $\text{H}_2\text{O} + \text{vinyl}$ products, which quickly dissociate. In order for this abstraction to occur, a barrier of about 6 kcal/mol (relative to this region of the PES) must be overcome. Analysis of the trajectories indicates that two types of motion are particularly effective in overcoming this barrier, namely, internal rotational energy imparted to the OH fragment and vibrational excitation of the bending modes of C_2H_4 .

Two representative trajectories are illustrated in Figure 3, which shows the $r(\text{C}-\text{O})$ bond distance and the kinetic energy of the OH fragment during the part of the trajectory where water is formed. The total lengths of the trajectories are 10 and 12 ps, respectively. During several periods before the reaction commences, the average distance of the C–OH stretch and the average kinetic energy in the OH fragment remain fairly constant. In the middle period, the OH has partially detached and is in the region of the hydrogen-bonded complex from which it starts to get pulled back toward the ethene at the end of the trajectory. While the OH is distant from the ethene, the

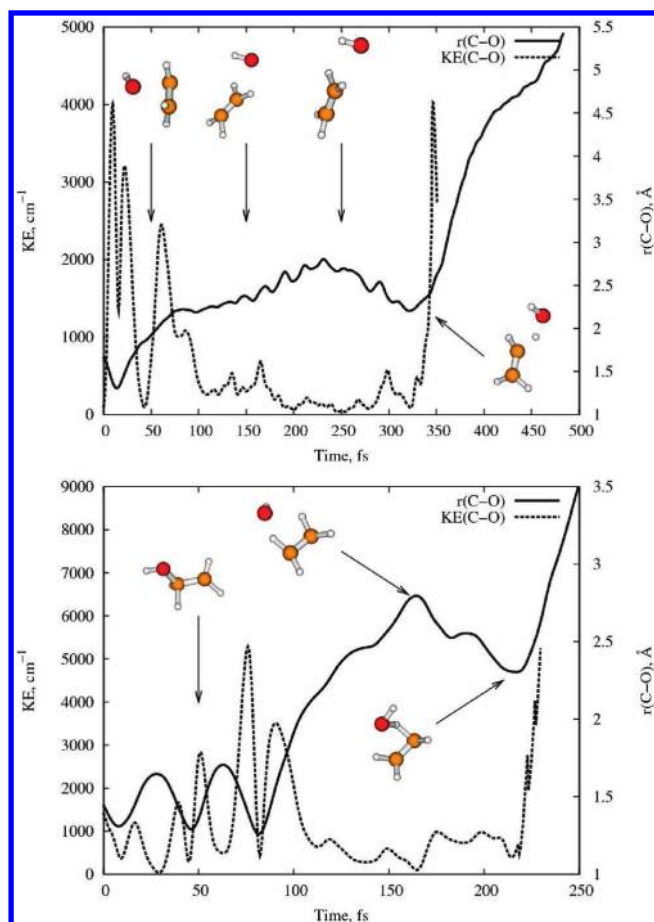


Figure 3. Kinetic energy in the C–O bond stretch and $r(\text{C}-\text{O})$ bond length during two H_2O loss events. In the top trajectory, until $t = 0 \text{ fs}$, the OH fragment undergoes normal oscillations for about 10 ps. From $t = 50$ to 300 fs, the OH fragment begins to move away and enters a region of increased $r(\text{C}-\text{O})$ bond length and decreased vibrational kinetic energy until at $t = 350 \text{ fs}$, the OH abstracts a hydrogen from the same carbon from which it dissociated to form water + vinyl. In the bottom trajectory, after 12 ps, the OH fragment roams from $t = 100$ to 200 fs when it abstracts a hydrogen from the other carbon and dissociates.

ethene can rotate almost independently, and therefore, when the OH is finally pulled back, the orientation is favorable for abstraction to form water, as evidenced in the last portion of the trajectory. The roaming part of the trajectories lasts a couple of hundred femtoseconds, similar to the case of formaldehyde. While there are two barriers in the dissociation of $\text{CH}_2\text{CH}_2\text{OH}$ to OH,⁴⁸ we find that it is only the inner barrier, associated with TS1, rather than the outer barrier (between M2 and P1) that plays an important role in the subsequent OH + ethene abstraction. This can be justified by geometric considerations since at the minimum M2, $r(\text{C}-\text{O})$ is 0.5 \AA longer than necessary for access to the abstraction TS and the OH orientation is wrong.

In order for the trajectory to form water, OH and ethene must transition from the region of phase space corresponding to complex formation to the region favorable to the abstraction TS. With energies in the C–O vibrational mode near the threshold for dissociation, OH can spend an extended amount

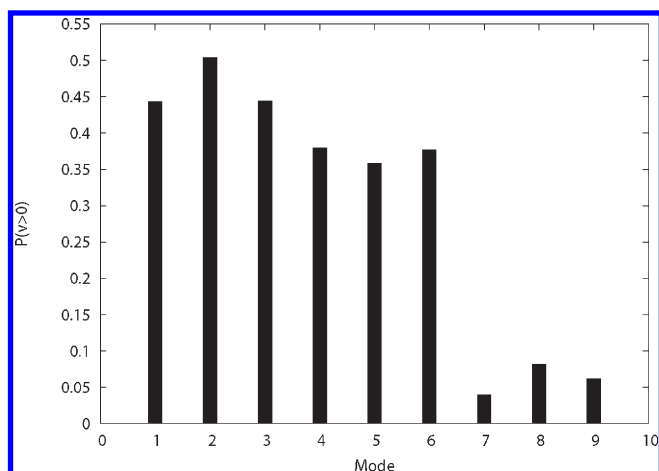


Figure 4. Fraction of vinyl produced with $\nu > 0$ in a specified normal mode of vinyl ordered according to ascending energy (in cm^{-1} , the frequencies are 730, 850, 965, 1077, 1419, 1689, 3118, 3222, and 3298). The fraction is calculated as the sum of all product states with $\nu > 0$ in a particular mode divided by the total number of product states. The low-frequency bending modes show considerable excitation, whereas the stretching modes remain relatively unexcited. The probabilities do not sum to unity because product states typically have excitations in multiple modes.

of time at C–O bond distances close to both TS1 and TS5. This allows for two types of reorientation to occur, independent rotation of the two fragments and out-of-plane excursions of the hydrogen atoms due to vibrational energy in the bending modes of ethene. The reorientation is partially facilitated by the flatness of the PES in this region. Changes in the dihedral angle defining the direction that OH points relative to ethene result in almost no change to the potential energy over a wide range of angles. As long as the hydrogen is pointing somewhat into the π cloud of ethene, there is still a favorable interaction which holds the hydrogen-bonded complex together. TS5 also appears to be somewhat loose with regard to similar motions, which increases the likelihood of a roaming OH finding the correct geometry to abstract the hydrogen. This flexibility is important in allowing kinetic energy from several different sources to contribute to overcoming the barrier. A harmonic final state analysis of the vinyl fragment shows considerable vibrational excitation in the low-frequency bending modes, with only a small excitation in the stretching modes (Figure 4). The distorted geometry of the water in TS5 leads to excitation of its bending and asymmetric stretch modes.

The initial rotational impulse imparted to OH before it begins roaming determines from which carbon the OH finally abstracts the hydrogen. There appears to be a slight preference for abstracting from the same carbon to which the oxygen was attached (approximately 54% of trajectories) as opposed to the other carbon (46% of trajectories). The two types of trajectories shown in Figure 3 are representative of those leading to abstraction from the same (top) and from opposing (bottom) carbons. In the top trajectory, the internal energy is primarily located in vibrational motion associated with the C–O stretch, and the nascent OH fragment is formed with small rotational energy. In contrast, the second trajectory has the OH possessing a large rotational component and only

the minimum required in the vibrational coordinate, propelling it toward the second carbon. (Movies of both trajectories are available as Supporting Information.)

Quasiclassical trajectories are known to have problems with conservation of ZPE because the energy originally present as ZPE is free to be redistributed during the course of the trajectory. We have ignored trajectories leading to pairs of products that do not contain enough internal energy to satisfy the respective zero-point requirements for each. Throwing away these trajectories decreases the relative yield of $\text{H}_2\text{O} + \text{vinyl}$ because more trajectories leading to $\text{H}_2\text{O} + \text{vinyl}$ violate ZPE than trajectories leading to other products. However, in both cases, the branching is small (1.6% keeping all trajectories versus 1.2%). The redistribution of ZPE into other vibrational modes also allows for the observation of products below their calculated thresholds. For instance, the observed threshold for water formation is near the TS5 barrier height of 30.50 kcal/mol. However, because classical dynamics allows ZPE to “leak” out of normal modes, a small amount of water formation can still be observed somewhat below the energetic barrier. The overall branching to water formation is somewhat sensitive to the heights of different barriers as well as the exact fitting parameters used. Although there was considerable variation within different versions of the potential, the two types of trajectories shown in Figure 3 were consistently seen, and the water channel was always observed. On the PES reported here, branching to water loss represented approximately 1% of the overall products, comparable to the formation of the $\text{H} + \text{CH}_2\text{CHOH}$ channel (P2), which was recently observed experimentally.⁴⁰

The evolution of the HOMO reveals that water loss involves the creation of two distinct species and therefore is not a concerted process. Figure 5 shows the evolution of the HOMO during one trajectory leading to water formation. The two upper panels depict the early parts of the trajectory. The HOMO at the starting geometry (panel a) can be described as a lone pair p orbital on the carbon not bonded to oxygen with contributions from the σ -bonding CH part (between the other carbon and each of its hydrogens) and the lone pair on the oxygen.

In the lower left-hand corner (Figure 5c), which corresponds to the part of the trajectory where the OH group is roaming, the HOMO has a clear π -like character on the ethene fragment as well as the lone pairs on oxygen. This picture indicates that the C–O bond has formally been broken and that the hydroxyl is far enough away to be considered a separate species. The attractive hydrogen-bonding interaction between the H of OH and the π cloud of ethene, however, is sufficient to prevent the two fragments from falling apart and eventually leads to their final approach in the lower right-hand corner (Figure 5d) to form water plus vinyl. As the OH leaves, the ethene flattens, rotating the C–H σ -orbitals into the plane of the ethene. When it moves further away, the HOMO on ethene continues to rotate, eventually forming the π system of ethene.

This paper presents a theoretical study that predicts a roaming-type mechanism for the production of water + vinyl, which is inaccessible at the available energy used here via direct predissociation of the 2-hydroxyethyl radical.

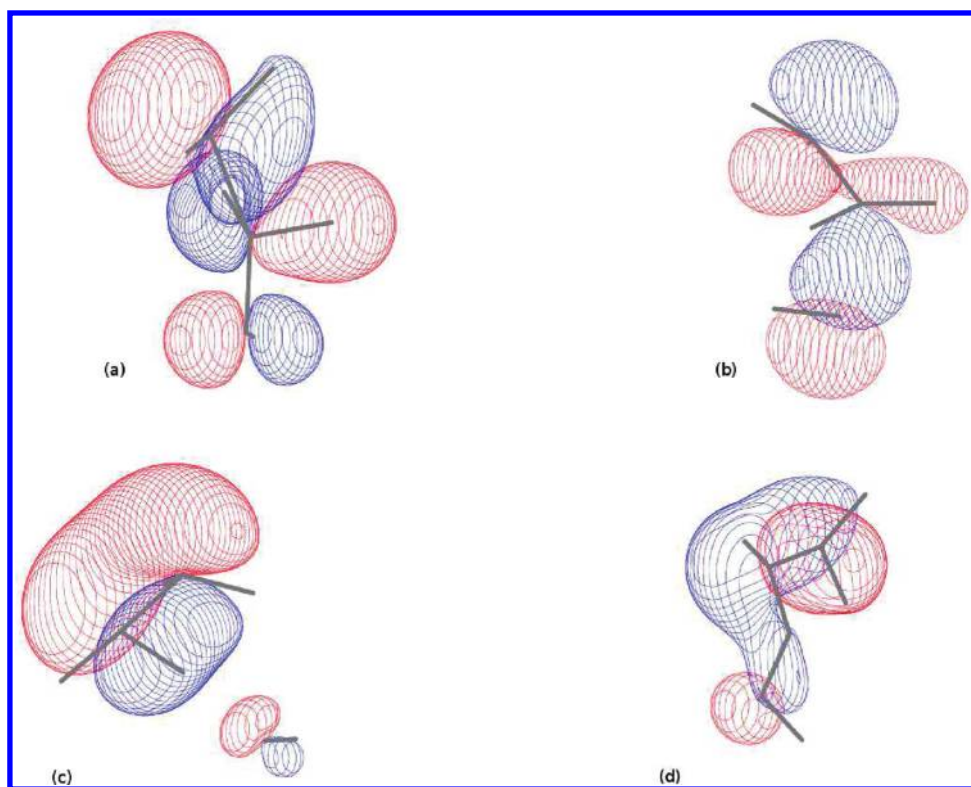


Figure 5. The evolution of the HOMO during a trajectory leading to H_2O . The initial $\text{CH}_2\text{CH}_2\text{OH}$ HOMO (top-left) is rotated into the π -like orbital of ethene as the OH fragment leaves (top-right and bottom-left), until the lone pair on the OH fragment is able to interact with and abstract a hydrogen from ethene (bottom-right).

We demonstrate that this channel proceeds through frustrated ethene + OH dissociation. The existence of the weakly bound $\text{CH}_2\text{CH}_2\text{-OH}$ complex in the product channel enables the roaming OH to find a favorable orientation to abstract a hydrogen from ethene. Interestingly, the trajectories indicate that hydrogen can be abstracted from either the 1 or 2 carbons. The presence of the complex at relatively large fragment separations serves to frustrate fast and direct dissociation and allows a small fraction of the dissociating molecules to access parts of the PES, leading to abstraction of a hydrogen by the departing OH.

There are two interesting features that have not been previously considered in the roaming discussion. First, the roaming involves a reaction between a closed-shell molecule (ethene) and a radical (hydroxyl). Second, we show that the small barrier to the abstraction can be overcome by rovibrational motions in the fragments. While such events represent a particularly fortunate confluence of circumstances, that is, near-dissociation threshold energy in the C–O vibrational mode as well as the correct phase and partitioning of energy into vinyl bending modes, they still posit the existence of a previously unexplored channel.

The goal of the present paper was to establish the roaming mechanism under a set of conditions that is close to what can be achieved experimentally. While the PES is not yet sufficiently accurate to predict quantitative branching ratios, small variations in relative barrier heights do not eliminate the roaming channel. In the future, we plan to refine the PES,

as well as study the influence on branching ratios of specific modes of rovibrational excitation in the radical. In addition, the roles of the binding in the hydrogen-bonded complex and the abstraction reaction barrier height will be explored.

Importantly, this work suggests that mechanisms such as roaming may allow access to reaction pathways that classical TS theory may exclude. In this case, direct water loss would involve a TS that is energetically inaccessible, and therefore, the only pathway leading to water formation is roaming. While our calculations suggest that the branching to this channel is small, the formation of water is persistent, and we predict that it could be observed in experiments with sufficient sensitivity. In fact, enhancement in the 121.56 nm laser ionization signal at the mass of the deuterated vinyl radical has recently been observed by Reisler and co-workers in the 202–207 nm photolysis of $\text{BrCD}_2\text{CD}_2\text{OH}$, but its origin could not be definitively attributed to the secondary dissociation of $\text{CD}_2\text{CD}_2\text{OH}$ (private communication). Vinyl products have been recently detected by Butler and co-workers from a nonthermal distribution of $\text{CH}_2\text{CH}_2\text{OH}$ radicals (produced by 193 nm photolysis of $\text{BrCH}_2\text{CH}_2\text{OH}$) with rovibrational energies above the OH + ethene entrance channel (private communication). We conclude, therefore, that roaming reactions involving small internal barriers to abstraction are possible, and in the future, we will explore the influence of different parameters such as barrier heights, geometry, and vibrational excitations in order to assess whether such channels can become significant contributors.

SUPPORTING INFORMATION AVAILABLE Description of the method used to construct the PES, comparisons of our PES with previously reported works, an energy level diagram indicating the position of connectivity of the relevant species, and two movies of sample trajectories. This material is available free of charge via the Internet at <http://pubs.acs.org>.

AUTHOR INFORMATION

Corresponding Author:

*To whom correspondence should be addressed.

ACKNOWLEDGMENT This work is conducted under the auspices of the iOpenShell Center for Computational Studies of Electronic Structure and Spectroscopy of Open-Shell and Electronically Excited Species supported by the National Science Foundation through the CRIF:CRF CHE-0625419+0624602+0625237 grant. A.I.K., J.M.B., and H.R. also acknowledge support of the Department of Energy (DE-FG02-05ER15685, DE-FG02-97ER14782, and DE-FG02-05ER15629, respectively).

REFERENCES

- Townsend, D.; Lahankar, S.; Lee, S.; Chambreau, S.; Suits, A.; Zhang, X.; Rheinecker, J.; Harding, L.; Bowman, J. The Roaming Atom: Straying from the Reaction Path in Formaldehyde Decomposition. *Science* **2004**, *306*, 1158–1161.
- Lahankar, S. A.; Goncharov, V.; Suits, F.; Farnum, J. D.; Bowman, J. M.; Suits, A. G. Further Aspects of the Roaming Mechanism in Formaldehyde Dissociation. *Chem. Phys.* **2008**, *347*, 288–299.
- Heazlewood, B. R.; Jordan, M. J. T.; Kable, S. H.; Selby, T. M.; Osborn, D. L.; Shepler, B. C.; Braams, B. J.; Bowman, J. M. Roaming is the Dominant Mechanism for Molecular Products in Acetaldehyde Photodissociation. *Proc. Natl. Acad. Sci. U.S.A.* **2008**, *105*, 12719–12724.
- Houston, P. L.; Kable, S. H. Photodissociation of Acetaldehyde as a Second Example of the Roaming Mechanism. *Proc. Natl. Acad. Sci. U.S.A.* **2006**, *103*, 16079–16082.
- Suits, A. G. Roaming Atoms and Radicals: A New Mechanism in Molecular Dissociation. *Acc. Chem. Res.* **2008**, *41*, 873–881.
- Osborn, D. L. Exploring Multiple Reaction Paths to a Single Product Channel. *Adv. Chem. Phys.* **2008**, *138*, 213–265.
- Bowman, J. M.; Shepler, B. C. Roaming Radicals. *Annu. Rev. Phys. Chem.* In press.
- van Zee, R. D.; Foltz, M. F.; Moore, C. B. Evidence for a Second Molecular Channel in the Fragmentation of Formaldehyde. *J. Chem. Phys.* **1993**, *99*, 1664–1673.
- Zhang, X.-B.; Zou, S.-L.; Harding, L.; Bowman, J. A Global ab Initio Potential Energy Surface for Formaldehyde. *J. Phys. Chem. A* **2004**, *108*, 8980–8986.
- Shepler, B.; Braams, B.; Bowman, J. Quasiclassical Trajectory Calculations of Acetaldehyde Dissociation on a Global Potential Energy Surface Indicate Significant Non-transition State Dynamics. *J. Phys. Chem. A* **2007**, *111*, 8282–8285.
- Shepler, B. S.; Braams, B. J.; Bowman, J. M. “Roaming” Dynamics in CH₃CHO Photodissociation Revealed on a Global Potential Energy Surface. *J. Phys. Chem. A* **2008**, *112*, 9344–9351.
- Harding, L. B.; Georgievskii, Y.; Klippenstein, S. J. Roaming Radical Kinetics in the Decomposition of Acetaldehyde. *J. Phys. Chem. A* **2010**, *114*, 765–777.
- Zhu, R. S.; Park, J.; Lin, M. C. Ab Initio Kinetic Study on the Low-Energy Paths of the HO + C₂H₄ Reaction. *Chem. Phys. Lett.* **2005**, *408*, 25–30.
- Senosiain, J.; Klippenstein, S.; Miller, J. Reaction of Ethylene with Hydroxyl Radicals: A Theoretical Study. *J. Phys. Chem. A* **2006**, *110*, 6960–6970.
- Liu, A.; Mulac, W. A.; Jonah, C. D. Kinetic Isotope Effects in the Gas-Phase Reaction of Hydroxyl Radicals with Ethylene in the Temperature Range 345–1173 K and 1-atm Pressure. *J. Phys. Chem.* **1988**, *92*, 3828–3833.
- Liu, G. X.; Ding, Y. H.; Li, Z. S.; Fu, Q.; Huang, X. R.; Sun, C. C.; Tang, A. C. Theoretical Study on Mechanisms of the High-Temperature Reactions C₂H₃ + H₂O and C₂H₄ + OH. *Phys. Chem. Chem. Phys.* **2002**, *4*, 1021–1027.
- Anastasi, C.; Simpson, V.; Munk, J.; Pagsberg, P. UV Spectrum and the Kinetics and Reaction Pathways of the Self-Reaction of Hydroxyethyl Radicals. *J. Phys. Chem.* **1990**, *94*, 6327–6331.
- Cool, T.; Nakajima, K.; Mostefaoui, T.; Qi, F.; McIlroy, A.; Westmoreland, P.; Poisson, L.; Peterka, D.; Ahmed, M. Selective Detection of Isomers With Photoionization Mass Spectrometry for Studies of Hydrocarbon Flame Chemistry. *J. Chem. Phys.* **2003**, *119*, 8356–8365.
- Chandler, D. W.; Thoman, J. W.; Hess, W. P. Photofragment Imaging: The Photodissociation of Bromomethane, Bromoethane, and Bromoethanol. *Inst. Phys. Conf. Ser.* **1991**, *114*, 355.
- Sapers, S. P.; Hess, W. P. Photodissociation of BrCH₂CH₂-OH and ICH₂CH₂OH: Formation and characterization of OH(X²Π). *J. Chem. Phys.* **1992**, *97*, 3126–3134.
- Shubert, V. A.; Rednic, M.; Pratt, T. S. Photodissociation of 2-Iodoethanol within the A Band. *J. Phys. Chem. A* **1992**, *113*, 9057–9064.
- Hintsä, E. J.; Zhao, X.; Lee, Y. T. Photodissociation of 2-Bromoethanol and 2-Chloroethanol at 193 nm. *J. Chem. Phys.* **1990**, *92*, 2280–2286.
- Vakhtin, A. B.; Murphy, J. E.; Leone, S. R. Low-Temperature Kinetics of Reactions of OH Radical with Ethene, Propene, and 1-Butene. *J. Phys. Chem. A* **2003**, *107*, 10055–10062.
- Yamada, T.; Bozzelli, J. W. Kinetic and Thermodynamic Analysis on OH Addition to Ethylene: Adduct Formation, Isomerization, and Isomer Dissociations. *J. Phys. Chem. A* **1999**, *103*, 7646–7655.
- Tully, F. Hydrogen-Atom Abstraction from Alkenes by OH, Ethene, and 1-Butene. *Chem. Phys. Lett.* **1988**, *143*, 510–514.
- Taatjes, C.; Hansen, N.; McIlroy, A.; Miller, J.; Senosiain, J.; Klippenstein, S.; Qi, F.; Sheng, L.; Zhang, Y.; Cool, T.; et al. Enols Are Common Intermediates in Hydrocarbon Oxidation. *Science* **2005**, *308*, 1887–1889.
- Karpichev, B.; Edwards, L. W.; W., J.; Reisler, H. Electronic Spectroscopy and Photodissociation Dynamics of the 1-Hydroxyethyl Radical CH₃CHOH. *J. Phys. Chem. A* **2008**, *112*, 412–418.
- Diau, E. W. G.; Lee, Y. P. Detailed Rate Coefficients and the Enthalpy Change of the Equilibrium Reaction OH + C₂H₄ → HOC₂H₄ Over the Temperature Range 544–673K. *J. Chem. Phys.* **1992**, *96*, 377–386.
- Taatjes, C. A.; Hansen, N.; Miller, J. A.; Cool, T. A.; Wang, J.; Westmoreland, P. R.; Law, M. E.; Kasper, T.; Kohse-Hoinghaus, K. Combustion Chemistry of Enols: Possible Ethenol Precursors in Flames. *J. Phys. Chem. A* **2006**, *110*, 3254–3260.
- Sosa, C.; Schlegel, H. B. Calculated Barrier Heights for OH + C₂H₂ and OH + C₂H₄ using Unrestricted Moeller–Plesset Perturbation Theory with Spin Annihilation. *J. Am. Chem. Soc.* **1987**, *109*, 4193–4198.
- Hippler, H.; Viskolcz, B. Addition Complex Formation vs. Direct Abstraction in the OH + C₂H₄ Reaction. *Phys. Chem. Chem. Phys.* **2000**, *2*, 3591–3596.

- (32) Tully, F. P. Laser Photolysis/Laser-Induced Fluorescence Study of the Reaction of Hydroxyl Radical with Ethylene. *Chem. Phys. Lett.* **1983**, *96*, 148–153.
- (33) Xu, Z. F.; Xu, K.; Lin, M. C. Ab Initio Kinetics for Decomposition/Isomerization Reactions of C₂H₅O Radicals. *Chem. Phys. Chem.* **2009**, *10*, 972–982.
- (34) Ratliff, B. J.; Womack, C. C.; Tang, X. N.; Landau, W. M.; Butler, L. J.; Szpunar, D. E. Modeling the Rovibrationally Excited C₂H₄OH Radicals from the Photodissociation of 2-Bromoethanol at 193 nm. *J. Phys. Chem. A* **2010**, *114*, 4934–4945.
- (35) Karpichev, B.; Koziol, L.; Diri, K.; Reisler, H.; Krylov, A. Electronically Excited and Ionized States of the CH₂CH₂OH Radical: A Theoretical Study. *J. Chem. Phys.* **2010**, *132*, 114308.
- (36) Cleary, P.; Romero, M.; Blitz, M.; Heard, D.; Pilling, M.; Seakins, P.; Wang, L. Determination of the Temperature and Pressure Dependence of the Reaction OH + C₂H₄ from 200–400 K using Experimental and Master Equation Analyses. *Phys. Chem. Chem. Phys.* **2006**, *8*, 5633–5642.
- (37) Curtiss, L.; Lucas, D.; Pople, J. Energies of C₂H₅O and C₂H₅O⁺ Isomers. *J. Chem. Phys.* **1995**, *102*, 3292–3300.
- (38) Bock, C. W.; George, P.; Glusker, J. P. Ab-Initio Molecular-Orbital Studies on C₂H₅O⁺ and C₂H₄FO⁺ — Oxonium Ion, Carbocation, Protonated Aldehyde, and Related Transition-State Structures. *J. Org. Chem.* **1993**, *58*, 5816–5825.
- (39) Nobes, R. H.; Rodwell, W. R.; Bouma, W. J.; Radom, L. The Oxygen Analog of the Protonated Cyclopropane Problem. A Theoretical Study of the C₂H₅O⁺ Potential Energy Surface. *J. Am. Chem. Soc.* **1981**, *103*, 1913–1922.
- (40) Edwards, L. W.; Ryazanov, M.; Reisler, H.; Klippenstein, S. J. D-Atom Products in Predissociation of CD₂CD₂OH from the 202–215 nm Photodissociation of 2-Bromoethanol. *J. Phys. Chem. A* **2010**, *114*, 5453–5461.
- (41) Villa, J.; Gonzalez-Lafont, A.; Lluch, J. M.; Corchado, J. C.; Espinosa-Garcia, J. Understanding the Activation Energy Trends for the C₂H₄ + OH → C₂H₄OH Reaction By Using Canonical Variational Transition State Theory. *J. Chem. Phys.* **1997**, *107*, 7266–7274.
- (42) Sekusak, S.; Liedl, K. R.; Sabljic, A. Reactivity and Regioselectivity of Hydroxyl Radical Addition to Haalgenated Ethenes. *J. Phys. Chem. A* **1998**, *102*, 1583–1594.
- (43) Zhang, Y.; Zhang, S.; Li, Q. A Theoretical Study on the β-C-H Fission of Ethoxy Radical. *Chem. Phys.* **2004**, *296*, 79–86.
- (44) Zhang, Y.; Zhang, S.; Li, Q. Ab initio Calculations and Mechanism of Two Proton Migration Reactions of Ethoxy Radical. *Chem. Phys.* **2005**, *308*, 109–116.
- (45) Shao, Y.; Molnar, L. F.; Jung, Y.; Kussmann, J.; Ochsenfeld, C.; Brown, S.; Gilbert, A. T. B.; Slipchenko, L. V.; Levchenko, S. V.; O'Neil, D. P.; et al. Advances in Methods and Algorithms in a Modern Quantum Chemistry Program Package. *Phys. Chem. Chem. Phys.* **2006**, *8*, 3172–3191.
- (46) Braams, B. J.; Bowman, J. M. Permutationally Invariant Potential Energy Surfaces in High Dimensionality. *Int. Rev. Phys. Chem.* **2009**, *28*, 577–606.
- (47) MOLPRO 2002.6.; Werner, H.-J.; Knowles, P.; Lindh, R.; Schütz, M.; et al.; Cardiff, UK, 2003; <http://www.molpro.net>.
- (48) Greenwald, E. E.; North, S. W.; Georgievskii, Y.; Klippenstein, S. J. A Two Transition State Model for Radical–Molecule Reactions: A Case Study of the Addition of OH to C₂H₄. *J. Phys. Chem. A* **2005**, *109*, 6031–6044.